Characterization of wild-type and STAT3 signaling-suppressed mesenchymal stem cells obtained from hemovac blood concentrates

Dong Hwan Lee[1], Seon Ae Kim[1], Eun Jeong Go[1], Chi Young Yoon[1], Mi-La Cho[2], Asode Ananthram Shetty[3], Seok Jung Kim[1]

[1]Department of Orthopedic Surgery, College of Medicine, The Catholic University of Korea, Seoul, Republic of Korea; [2]The Rheumatism Research Center, Catholic Research Institute of Medical Science, College of Medicine, The Catholic University of Korea, Seoul, Republic of Korea; [3]Institute of Medical Sciences , Faculty of Health and Social Care, Canterbury Christ Church University, Kent, UK

Contributions: (I) Conception and design: ML Cho, SJ Kim; (II) Administrative support: CY Yoon; (III) Provision of study materials or patients: EJ Go; (IV) Collection and assembly of data: SA Kim; (V) Data analysis and interpretation: DH Lee, AA Shetty; (VI) Manuscript writing: All authors; (VII) Final approval of manuscript: All authors.

Correspondence to: Seok Jung Kim, MD, PhD, FRCS. Department of Orthopedic Surgery, Uijeongbu St. Mary's Hospital, College of Medicine, The Catholic University of Korea, 271, Cheonbo-ro, Uijeongbu-si, Gyeonggi-do, 11765, Republic of Korea. Email: peter@catholic.ac.kr.

Background: Venous blood drained from the knee joint after total knee arthroplasty (TKA) using a hemovac line is a potential source of bone marrow components, including stem cells, from the cutting surface of cancellous bones of the knee joint. However, the function of mesenchymal stem cells (MSCs) in patients with osteoarthritis (OA-MSCs) can be disrupted by inflammation of the joint. Further, to override the invasive nature of the currently used methods to obtain stem cells, their functional modification is necessary for therapeutic applications.

Methods: The effects of signal transducer and activator of transcription 3 (STAT3) signaling suppression on MSCs (iSTAT3-MSCs) were evaluated by comparative analyses of the characteristics of OA-MSCs and iSTAT3-MSCs from 20 patients who underwent TKA.

Results: OA-MSCs and iSTAT3-MSCs were adherent, with fibroblast-like appearance and high rates of expression of MSC-specific markers, including CD73, CD90, and CD105 (>90%). Both OA-MSCs and iSTAT3-MSCs were able to differentiate into osteogenic, adipogenic, and chondrogenic cells; however, iSTAT3-MSCs showed higher levels of osteogenic and chondrogenic differentiation markers than OA-MSCs. Additionally, the anti-inflammatory and chondroprotective cytokine levels were higher in iSTAT3-MSCs than in OA-MSCs.

Conclusions: These findings indicate that iSTAT3-MSCs after TKA are potentially effective for stem cell therapy in the context of bone and cartilage disorders.

Keywords: Total knee arthroplasty (TKA); hemovac; osteoarthritis (OA); signal transducer and activator of transcription 3 (STAT3); stem cell therapy

Introduction

Total knee arthroplasty (TKA) is the gold standard treatment for end-stage osteoarthritis (OA); a large number of patients undergo this procedure every year (1-6). A large amount of venous blood in the knee joint after TKA surgery can cause pain, swelling, and delayed recovery (7-11). A hemovac line can be inserted into the joint to drain the blood and reduce joint pressure (12-14). Bone marrow
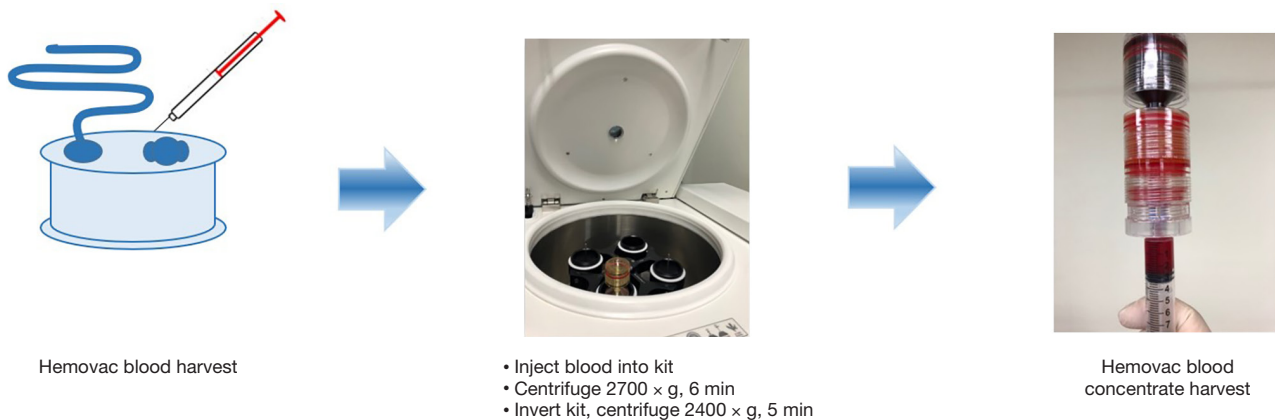
Page 2 of 14

Lee et al. STAT3 suppression in MSCs from HVB

Hemovac blood harvest

• Inject blood into kit
• Centrifuge 2700 × g, 6 min
• Invert kit, centrifuge 2400 × g, 5 min

Hemovac blood concentrate harvest

Figure 1 Overview of the procedure used to obtain hemovac blood concentrates.

components from the cutting surface of cancellous bones of the distal femur and proximal tibia can be found in hemovac blood (HVB) (e.g., stromal cells, including stem cells) (15,16). As HVB is mostly venous blood, stromal components from the bone marrow must be isolated from HVB concentrates (HVBCs) by centrifugation (17). Importantly, stem cells isolated from HVB are multipotent, with the ability to differentiate into osteogenic, adipogenic, and chondrogenic cells (17).

However, patients who undergo TKA are typically elderly and/or have inflammatory joint conditions (18,19). Consequently, their stem cells express inflammatory signals (20,21). Therefore, to use HVB from such patients for stem cell therapy, it is necessary to modify MSCs aiming to reduce the expression of inflammatory factors.

We hypothesized that the inhibition of signal transducer and activator of transcription 3 (STAT3) in MSCs derived from HVB collected from patients subjected to TKA would improve their functions in the context of OA. Therefore, in this study, to improve the therapeutic potential of MSCs, we treated OA-MSCs with STA21, a STAT3 inhibitor. The anti-inflammatory effects, marker expression, and the differentiation ability of MSCs (wild type *vs.* STA21-treated) were then evaluated *in vitro*. We present the following article in accordance with the MDAR reporting checklist (available at https://dx.doi.org/10.21037/atm-21-791).

Methods

Patients and ethical statement

HVB was collected from 20 patients who underwent TKA.

The average age of the patients was 51.2 years [range, 38–66 years; standard deviation (SD), 7.52]. The study was conducted in accordance with the Declaration of Helsinki (as revised in 2013) and approved by the Institutional Review Board of Uijeongbu St. Mary's Hospital, Seoul, Korea (UC18DESI0056). Informed consent was provided by all patients prior to sample collection.

Isolation and culture of OA-MSCs from HVBCs

Just before wound closure, a hemovac line was inserted through the superolateral aspect of the patella and placed in the lateral gutter of the knee joint. The line was connected to the hemovac and an average of 300 mL blood was collected within 3 h after surgery.

HVB (40 mL), including 4 mL of ACD solution, was aseptically aspirated from the hemovac after TKA. The BMC Kit (Revmed, Seongnam, Korea) was used to concentrate the blood aspirate via two cycles of centrifugation (*Figure 1*). HVBCs and PBS (Gibco Invitrogen, Grand Island, NY, USA) were then mixed at a 1:2 ratio. The mixture was carefully loaded on the top of Histopaque solution (1.077 g/m; Sigma Chemical co., St. Louis, MO, USA). Mononuclear cells were separated by density gradient centrifugation (400 ×g, 25 min, room temperature), washed three times with PBS, and filtered using a 70-μm cell strainer (Becton Dickinson, Franklin Lakes, NJ, USA). Resuspended cells were incubated at 37 ℃ with 5% CO_2 in basal medium (αMEM containing 10% FBS, 100 units/mL penicillin, and 100 μg/mL streptomycin). The medium was changed at 3-day intervals and non-adherent cells were removed by gently pipetting.

The confluent cells were trypsinized (0.25% trypsin EDTA), divided into several culture flasks, expanded by passaging (2–3 passages), and used for experiments as OA-MSCs.

Inhibition of STAT3 signaling in MSCs (iSTAT3-MSCs)

iSTAT3-MSCs were obtained by adding 10 µM STA21 (Santa Cruz Biotechnology, Dallas, TX, USA) to OA-MSCs for 72 h.

Enzyme-linked immunosorbent assay (ELISA)

The concentrations of IL-6 (DY206-05; R&D Systems, Minneapolis, MN, USA), IL-8 (DY206, RRID: AB_2814717; R&D Systems), IL-1β (DY201-05; R&D Systems), IL-10 (DY217B-05; R&D Systems), TGF-β (DY240-05; R&D Systems), and vascular endothelial growth factor (VEGF; DY293B-05; R&D Systems) were measured in the culture supernatants of OA-MSCs and iSTAT3-MSCs using commercial ELISA kits, according to the manufacturer's instructions.

Flow cytometry

The surface markers of OA-MSCs and iSTAT3-MSCs were analyzed using a FACSCalibur Flow Cytometer (BD Biosciences, San Jose, CA, USA). Briefly, the harvested cells were fixed in 4% paraformaldehyde at 4 ℃ for 30 min and washed in cold flow cytometry buffer (BD Biosciences). Aliquots of 1×10^6 cells were incubated with specific antibodies for 20 min in the dark. After incubation, the cells were washed in PBS, and the expression of the different surface markers was assessed by flow cytometry.

The antibodies used in this study were: anti-CD73 (ecto-5'-nucleotidase; Phycoerythrin (PE)-labeled mouse anti-human CD73, clone AD2, 550257, BD Biosciences, Heidelberg, Germany), anti-CD90 (thy-1; allophycocyanin (APC)-labeled mouse anti-human CD90, clone 5E10, 17-0909, eBioscience, Waltham, MA, USA), anti-CD105 (Endoglin; PE-labeled mouse anti-human CD105, clone 266, 560839, BD Biosciences), anti-CD34 (hematopoietic progenitor cell antigen CD34; Fluorescein isothiocyanate (FITC)-labeled mouse anti-human CD34, clone 581, 560942, BD Biosciences), anti-CD45 (leukocyte common antigen; PE-labeled mouse anti-human CD45, clone HI30, 555483, BD Biosciences), HLA-DR (MHC class II antigen; FITC-labeled mouse anti-human HLA-DR, clone G46-6,

555811, BD Biosciences). The corresponding isotype controls were also used: PE-labeled mouse IgG1, k (clone MOPC-21, 555749, BD Biosciences), APC-labeled mouse IgG1, k (clone P3.6.2.8.1, 17-4714, eBioscience) and FITC-labeled mouse IgG1, k (clone MOPC-21, 555748, BD Biosciences).

Quantitative real-time polymerase chain reaction

Total RNA was extracted from OA-MSCs and iSTAT3-MSCs using the RNeasy Mini Kit (74104; QIAGEN, Hilden, Germany). The RNA samples (≥20 ng/µL) were reverse transcribed into cDNA using the QuantiTect Reverse Transcription Kit (205311, Qiagen) following the manufacturer's instructions. All samples were then subjected to qPCR using SYBR Green (A6001; Promega, Madison, WI, USA) and the Promega qPCR system. The relative expression levels were determined using the $2^{-\Delta\Delta Ct}$ method. The sequences of primers were used: for *RUNX2*, 5'-CCG GTC TCC TTC CAG GAT-3', reverse 5'-GGG AAC TGC TGT GGC TTC-3'; for ALP, 5'-CCT TGA AAA ATG CCC TGA AA-3', reverse 5'-CTT GGA GAG AGC CAC AAA GG-3'; for osteocalcin, 5'-CCT TCA TGT CCA AGC AGG A-3', reverse 5'-GGC GGT CTT CAA GCC ATA C-3'; for osteopontin, 5'-CCT CCC GGT GAA AGT GAC-3', reverse 5'-CTG TGG CGC AAG GAG ATT-3'; for *C/EBPa*, 5'-TGC GCA AGA GCC GGG ACA AG-3', reverse 5'-ACC AGG GAG CTC TCG GGC AG-3'; for *PPARγ*, 5'-TGG AGC CTA AGT TTG AGT TTG-3', reverse 5'-ATC TTC TGG AGC ACC TTG G-3'; for *SOX9*, 5'-AGG AAG TCG GTG AAG AAC GG-3', reverse 5'-AAG TCG ATA GGG GGC TGT CT-3'; for aggrecan, 5'-AGT CAC ACC TGA GCA TC-3', reverse 5'-TCT GCG TTT GTA GGT GG-3'; for type II collagen, 5'-GTT CAC GTA CAC TGC CCT GA-3', reverse 5'-TGA CCC TCA AAC TCA TGC CTC-3'.

Evaluation of the differentiation potential of OA-MSCs and iSTAT3-MSCs

The osteogenic, adipogenic, and chondrogenic differentiation potential of OA-MSCs and iSTAT3-MSCs were evaluated. OA-MSCs and iSTAT3-MSCs were plated at a density of 2×10^4 cells/well in 6-well plates.

For osteogenic differentiation, cells were incubated in osteogenic medium (A1007201; Gibco, Life Technologies, Karlsruhe, Germany); the medium was changed every 2–3 days. After 14 days of culture, cells were washed thrice with
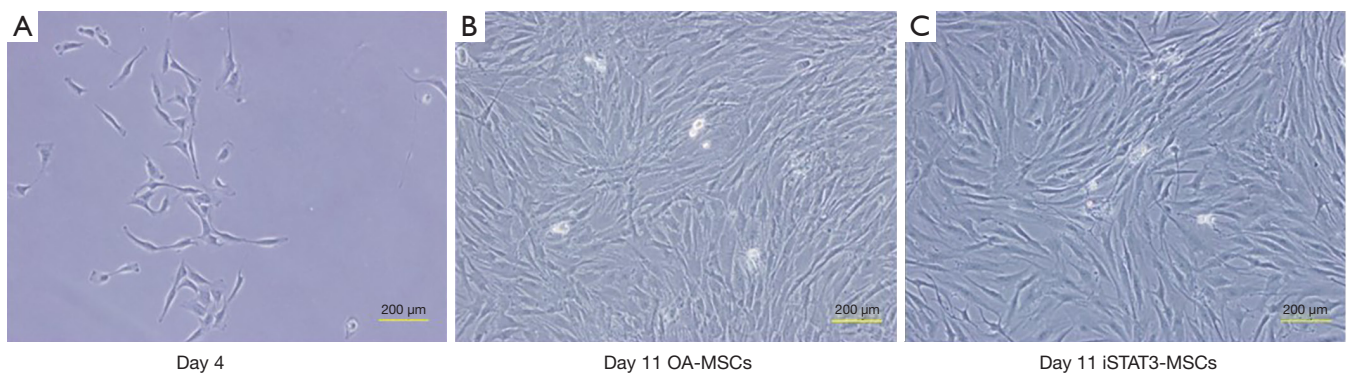
Page 4 of 14

Lee et al. STAT3 suppression in MSCs from HVB

Figure 2 Morphology of OA-MSCs and iSTAT3-MSCs. The morphology of OA-MSCs and iSTAT3-MSCs was observed under an microscope (BX51, Olympus, Tokyo, Japan), 4 (A) and 11 (B,C) days after *in vitro* culture. iSTAT3-MSCs attached to the well and showed no morphological differences from OA-MSCs. Scale bar =200 μm. OA-MSCs, mesenchymal stem cells in patients with osteoarthritis; STAT3, signal transducer and activator of transcription 3.

PBS (Gibco) and fixed in 4% paraformaldehyde at 4 ℃ for 20 min. The mineralization of the extracellular matrix as an indicator of osteogenic differentiation was determined using Alizarin red S and alkaline phosphatase (ALP) staining.

For adipogenic differentiation, cells were incubated in adipogenic differentiation medium (A1007001; Gibco); the medium was changed every 2–3 days. After 14 days, the cells were washed 3 times with PBS (Gibco) and fixed in 4% paraformaldehyde at 4 ℃ for 20 min. The cells were then treated with the Oil red O dye to visualize the lipids. For quantitative measurement, Oil red O was dissolved in isopropanol, and the absorbance was measured at 520 nm.

For chondrogenic differentiation, a pellet culture method was used. Briefly, 2.5×10^5 cells (passage 3) were resuspended in chondrogenic differentiation medium (A1007101; Gibco) in 15 mL polypropylene tubes. After centrifugation at 500 ×g for 5 min for aggregation, the cells were incubated at 37 ℃ in a humidified atmosphere containing 5% CO_2. The aggregates were cultivated for 21 days, and the medium was changed every 2–3 days. On day 21, the cell pellets were fixed in 10% formalin and embedded in paraffin. Then, 4-μm-thick tissue sections were obtained and stained with type II collagen (1:200, ab185430; Abcam, Cambridge, MA, USA), Alcian blue (pH 2.5), and toluidine blue to reveal the collagen and sulfated proteoglycan content in the extracellular matrix. Hematoxylin–eosin staining was also performed for morphological observations.

Statistical analysis

All statistical analyses were performed in triplicate. The results are shown as the mean ± standard deviation (SD). For comparison, the *t*-test and ANOVA were used (IBM SPSS, version 20.0). Statistical significance was defined as $P < 0.05$.

Results

Morphology of OA-MSCs and iSTAT3-MSCs

OA-MSCs were successfully isolated from HVBCs in all cases. The cells readily expanded *in vitro*, and fibroblast-like cells could be observed attached to the culture flasks, 4 to 8 days after initial plating (*Figure 2A*). The cells were maintained in αMEM supplemented with 10% FBS and penicillin. No morphological changes were observed after 11 days of culture (*Figure 2B*). Additionally, iSTAT3-MSCs showed no morphological differences (*Figure 2C*).

Expression of surface markers in OA-MSCs and iSTAT3-MSCs

The expression of different surface markers, including CD73, CD90, and CD105 (MSC-specific markers); CD34 (leukocyte common antigen cell marker); CD45 (hematopoietic stem cell marker); and HLA-DR (antigen-presenting cell marker), in OA-MSCs and iSTAT3-MSCs was evaluated by flow cytometry (*Figure 3*).

The expression of MSC-specific markers, including CD73 (95.2% in OA-MSCs and 97.8% in iSTAT3-MSCs), CD90 (91.6% in OA-MSCs and 94.3% in iSTAT3-MSCs), and CD105 (94.9% in OA-MSCs and 93.9% in iSTAT3-MSCs), was high (>90%) in both MSC types. However,
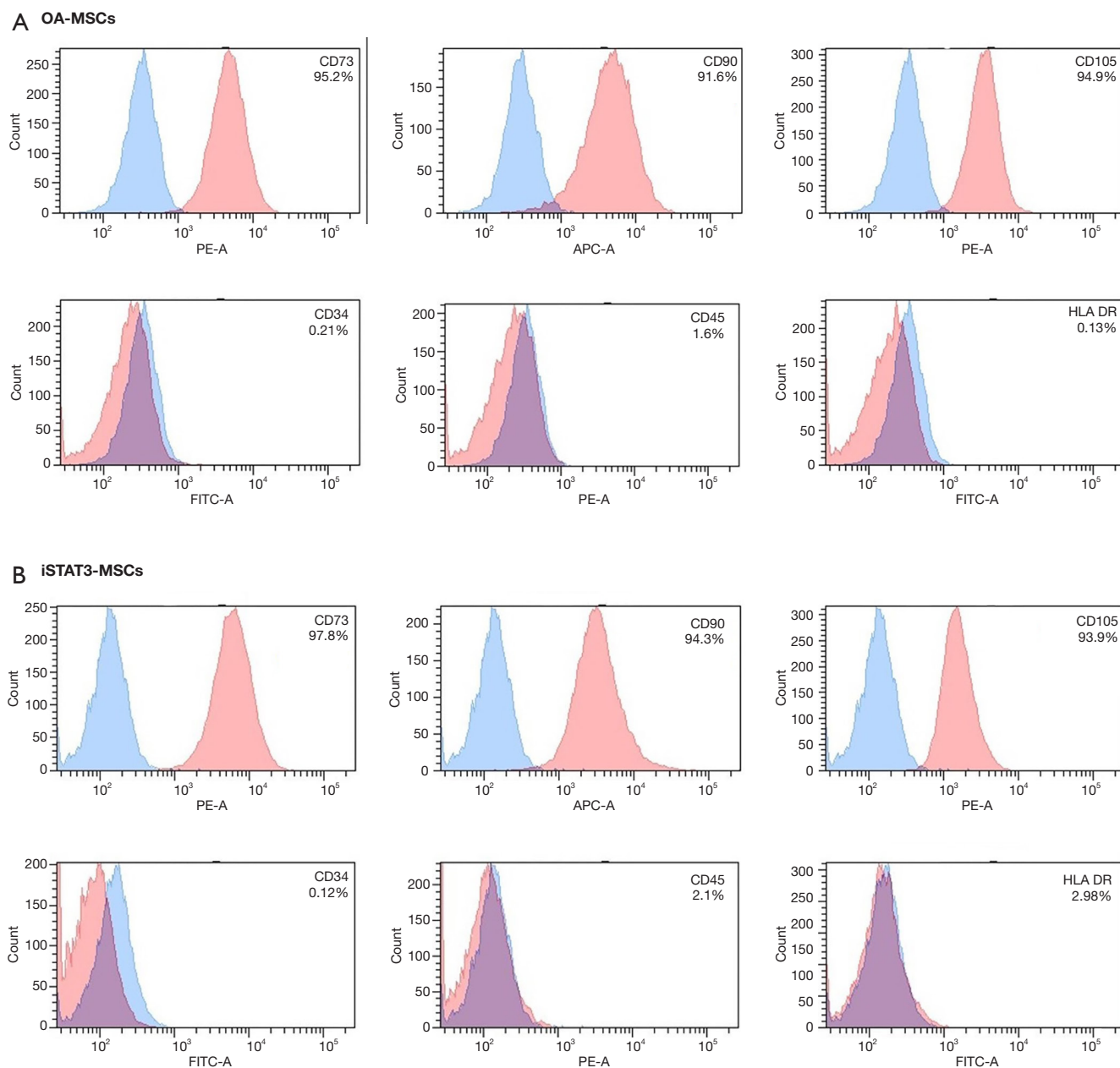
Figure 3 Expression of surface markers in OA-MSCs and iSTAT3-MSCs. (A) OA-MSCs; (B) iSTAT3-MSCs. The expression of the typical MSC markers—CD73, CD90, and CD105—was high (>90%) in both OA-MSCs and iSTAT3-MSCs. The negative markers—CD34, CD45, and HLA-DR—were barely expressed (<4%) in OA-MSCs and iSTAT3-MSCs. Blue: Isotype control expression. Red: Surface marker expression. OA-MSCs, mesenchymal stem cells in patients with osteoarthritis; STAT3, signal transducer and activator of transcription 3.

CD34 (0.21% in OA-MSCs and 0.12% in iSTAT3-MSCs), CD45 (1.6% in OA-MSCs and 2.1% in iSTAT3-MSCs), and HLA-DR (0.13% in OA-MSCs and 2.98% in iSTAT3-MSCs) expression was low (<4%). Notably, the surface marker expression profiles did not differ significantly between OA-MSCs and iSTAT3-MSCs.

Page 6 of 14

Lee et al. STAT3 suppression in MSCs from HVB

Multi-lineage differentiation (osteogenic, adipogenic, and chondrogenic) of OA-MSCs and iSTAT3-MSCs

Osteogenic differentiation was confirmed by determining the ALP and Alizarin red S staining after 14 days of culture (*Figure 4A,4B*). The ALP staining was not observed in undifferentiated OA-MSCs and iSTAT3-MSCs [*Figure 4A* (a and b)]. In contrast, differentiated OA-MSCs and iSTAT3-MSCs were stained purple [*Figure 4A* (c and d)]. As per the OD values, the ALP concentration was 1.397 ± 0.1623 U/mL in OA-MSCs and 1.684 ± 0.379 U/mL in iSTAT3-MSCs in the undifferentiated state and 7.189 ± 0.379 U/mL in OA-MSCs and 9.478 ± 0.455 U/mL in iSTAT3-MSCs in the differentiated state [*Figure 4A* (e)]. The OD values for the ALP assay were significantly different between OA-MSCs and iSTAT3-MSCs both in undifferentiated (*, $P<0.05$) and differentiated (**, $P<0.01$) states. Additionally, ALP concentrations differed significantly between undifferentiated and differentiated OA-MSCs (***, $P<0.001$) and iSTAT3-MSCs (***, $P<0.001$), with increased values in differentiated cells [*Figure 4A* (e)]. Undifferentiated OA-MSCs and iSTAT3-MSCs not observed mineral deposits [*Figure 4B* (a and b)]. In contrast, calcium deposition and mineralization were stained red in differentiated OA-MSCs and iSTAT3-MSCs [*Figure 4B* (c and d)]. Moreover, with respect to Alizarin red S staining the OD values were 0.04 ± 0.0006 nm for OA-MSCs and 0.044 ± 0.005 nm for iSTAT3-MSCs in the undifferentiated state and 0.159 ± 0.0014 nm for OA-MSCs and 0.171 ± 0.0038 nm for iSTAT3-MSCs in the differentiated state [*Figure 4B* (e)]. The OD values were not significantly different between undifferentiated OA-MSCs and iSTAT3-MSCs (#, $P>0.05$); however, they were significantly different between differentiated OA-MSCs and iSTAT3-MSCs (**, $P<0.01$). Additionally, the OD values were significantly different between undifferentiated and differentiated OA-MSCs (***, $P<0.001$) and iSTAT3-MSCs (***, $P<0.001$), with increased values in differentiated cells [*Figure 4B* (e)].

Adipogenic differentiation was observed by detecting intracellular lipids (stained in red) after Oil red O staining. Expectedly, lipid droplets were not found in undifferentiated OA-MSCs and iSTAT3-MSCs [*Figure 4C* (a and b)]. In contrast, intracellular lipid droplets were observed red in differentiated OA-MSCs and iSTAT3-MSCs [*Figure 4C* (c and d)]. The determined OD values were 0.368 ± 0.042 nm for OA-MSCs and 0.377 ± 0.058 nm for iSTAT3-MSCs in the undifferentiated state and 1.013 ± 0.077 nm for OA-MSCs and 1.066 ± 0.105 nm for iSTAT3-MSCs in the differentiated state [*Figure 4C* (e)]. Notably, the OD values were not significantly different between OA-MSCs and iSTAT3-MSCs in either condition (#, $P>0.05$). However, the OD values were significantly higher in differentiated than undifferentiated OA-MSCs and iSTAT3-MSCs [*Figure 4C* (e); ***, $P<0.001$].

Chondrogenic differentiation was observed using hematoxylin-eosin (to evaluate the cell morphology), Alcian blue (pH 2.5) and toluidine blue (to evaluate pericellular matrix proteoglycans), and type II collagen staining. Many round cells with a lacuna-like structure were observed in the context of OA-MSCs (*Figure 5A*; black arrow) and iSTAT3-MSCs (*Figure 5B*; red arrow) cultured in chondrogenic differentiation medium, as per hematoxylin-eosin staining. A rich extracellular matrix surrounding the cells was observed in both differentiated OA-MSCs and iSTAT3-MSCs. But, undifferentiated OA-MSCs and iSTAT3-MSCs not observed lacuna-like structure and round shape like chondrocytes (*Figure 5C,5D*). Differentiated OA-MSCs and iSTAT3 OA-MSCs showed strong Alcian blue (*Figure 5E*; black *, *Figure 5F*; red *), while undifferentiated OA-MSCs and iSTAT3-MSCs did not show any staining (*Figure 5G,5H*). In toluidine blue staining, differentiated OA-MSCs and iSTAT3 OA-MSCs showed strong purple (*Figure 5I*; yellow *, *Figure 5J*; yellow **), while undifferentiated OA-MSCs and iSTAT3-MSCs did not show staining (*Figure 5K,5L*). Notably, the Alcian blue (pH 2.5) and toluidine blue staining intensities were stronger in differentiated iSTAT3-MSCs (*Figure 5F,5J*) than OA-MSCs (*Figure 5E,5I*). Type II collagen is the main collagen component of the extracellular matrix in cartilage. Here, the expression of type II collagen in OA-MSCs (*Figure 5M*; black *) and iSTAT3-MSCs (*Figure 5N*; black **) was detected as brown color. In line with the above results, while type II collagen was not expressed in undifferentiated cells (*Figure 5O,5P*), the levels of type II collagen were detected in both differentiated iSTAT3-MSCs and OA-MSCs (to a greater extent in the former).

Gene expression analyses

The gene expression levels in OA-MSCs and iSTAT3-MSCs were evaluated on day 14 of culture after osteogenic and adipogenic differentiation and on day 21 after chondrogenic differentiation.

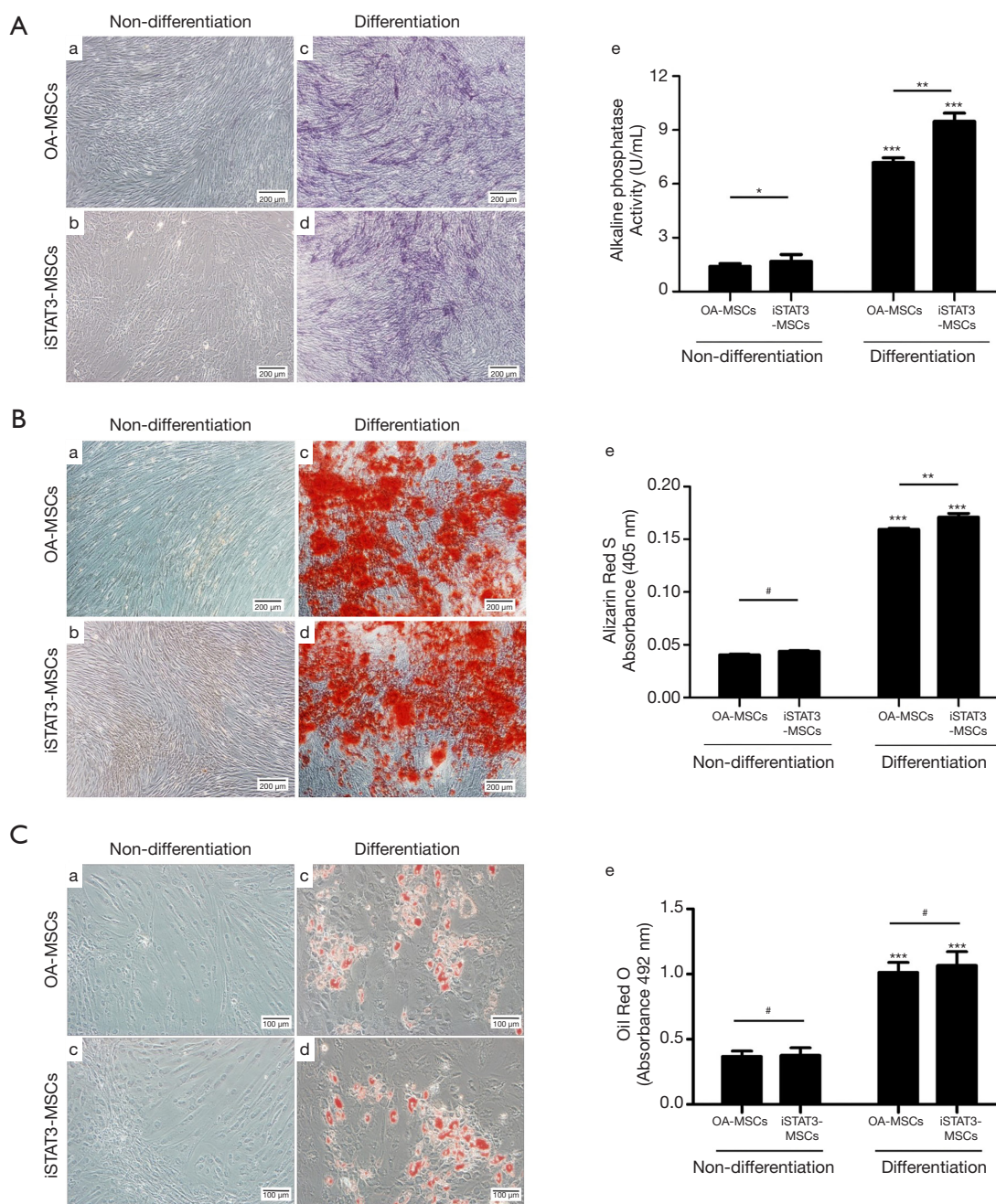Various osteogenic differentiation markers were

Figure 4 Osteogenic and adipogenic differentiation of OA-MSCs and iSTAT3-MSCs. [A (a-d)] Alkaline phosphatase was stained in blue. The activity of alkaline phosphatase was higher in differentiated than undifferentiated cells (blue in c and d; e; ***, P<0.001). A significant difference was also detected between OA-MSCs and iSTAT3-MSCs in both the undifferentiated and differentiated states (e; *, P<0.05 and **, P<0.01, respectively). Scale bar =200 μm. [B (a-d)] Calcium deposition was observed using Alizarin red S staining (red in c and d). Calcium deposition was higher in differentiated than undifferentiated cells (e; ***, P<0.001). The absorbance results were significantly different in the context of differentiated OA-MSCs than iSTAT3-MSCs (e; **, P<0.01) but not in the context of undifferentiated cells (#, P>0.05). Scale bar =200 μm. [C (a-d)] The Oil red O staining of lipid droplets is shown (red in c and d). The absorbance was higher in differentiated than undifferentiated cells (e; ***, P<0.001). In contrast, no significant differences were observed between OA-MSCs and iSTAT3-MSCs (e; #, P>0.05). Scale bar =100 μm. OA-MSCs, mesenchymal stem cells in patients with osteoarthritis; STAT3, signal transducer and activator of transcription 3.
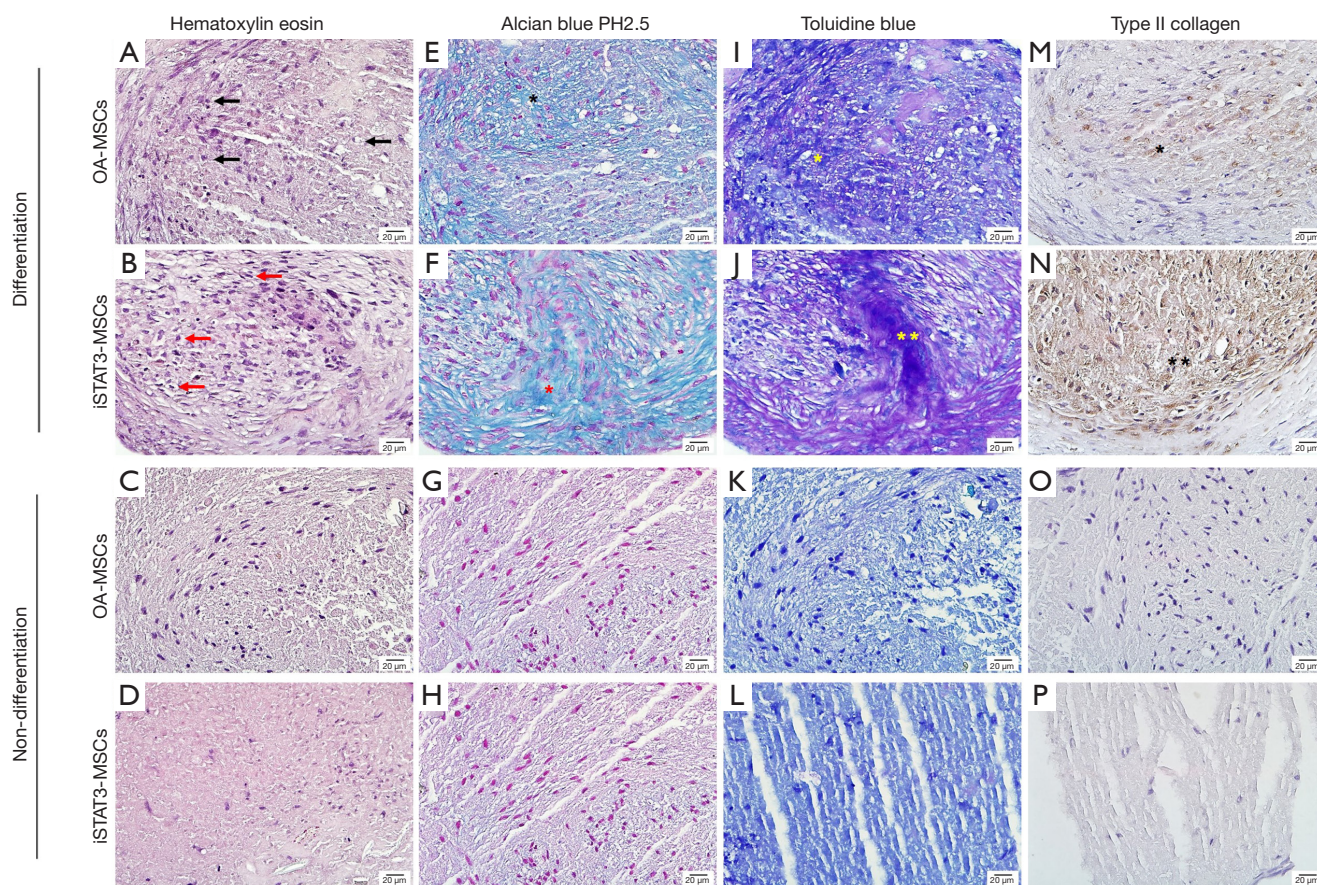
Page 8 of 14

Lee et al. STAT3 suppression in MSCs from HVB

Figure 5 Chondrogenic differentiation of OA-MSCs and iSTAT3-MSCs. Hematoxylin-eosin (A-D), Alcian blue pH 2.5 (E-H), toluidine blue (I-L), and type II collagen immunohistochemistry (M-P) staining images. Many cells aggregated to form a pellet. Chondrocyte-like cells with lacunae were observed in the differentiated state (A, black arrow; B, red arrow). Alcian blue (blue signals; E, black *; F, red *), toluidine blue (purple signals; I, yellow *; L, yellow **), and type II collagen (brown signals; M, black *; N, black **) staining indicated cartilage-like tissues in the differentiated state. The Alcian blue, toluidine blue, and type II collagen staining intensities were higher in the context of iSTAT3-MSCs than OA-MSCs in the differentiated state. Scale bar =20 μm. OA-MSCs, mesenchymal stem cells in patients with osteoarthritis; STAT3, signal transducer and activator of transcription 3.

evaluated. The expression of *RUNX2* was 1.92-fold and 2.18-fold higher in differentiated than undifferentiated OA-MSCs and iSTAT3-MSCs, respectively (*Figure 6A*; **, P<0.01). Additionally, the expression of *RUNX2* was higher in iSTAT3-MSCs than OA-MSCs in differentiated (*Figure 6A*; *, P<0.05). The expression of *ALP* was also 3.04-fold and 3.1-fold higher in differentiated than undifferentiated OA-MSCs and iSTAT3-MSCs, respectively (*Figure 6A*; **, P<0.01). However, *ALP* expression levels did not differ significantly between differentiated OA-MSCs and iSTAT3-MSCs (*Figure 6A*; #, P>0.05). The expression of osteocalcin was also 3.56-fold and 6.94-fold higher in differentiated than undifferentiated OA-MSCs and iSTAT3-MSCs,

respectively (*Figure 6A*; *, P<0.05). Additionally, the expression of osteocalcin was significantly higher in differentiated iSTAT3-MSCs than OA-MSCs (*Figure 6A*; ***, P<0.001). Moreover, the expression of osteopontin was 9.93-fold and 17.43-fold higher in differentiated than undifferentiated OA-MSCs and iSTAT3-MSCs, respectively (*Figure 6A*; ***, P<0.001); furthermore, it was significantly different between OA-MSCs and iSTAT3-MSCs in the differentiated state (*Figure 6A*; *, P<0.05).

With respect to adipogenic differentiation markers, the expression levels of *C/EBPα* and *PPARγ* were 2.71- and 3.23-fold higher, respectively, in differentiated than non-differentiated OA-MSCs; the same was true in the context
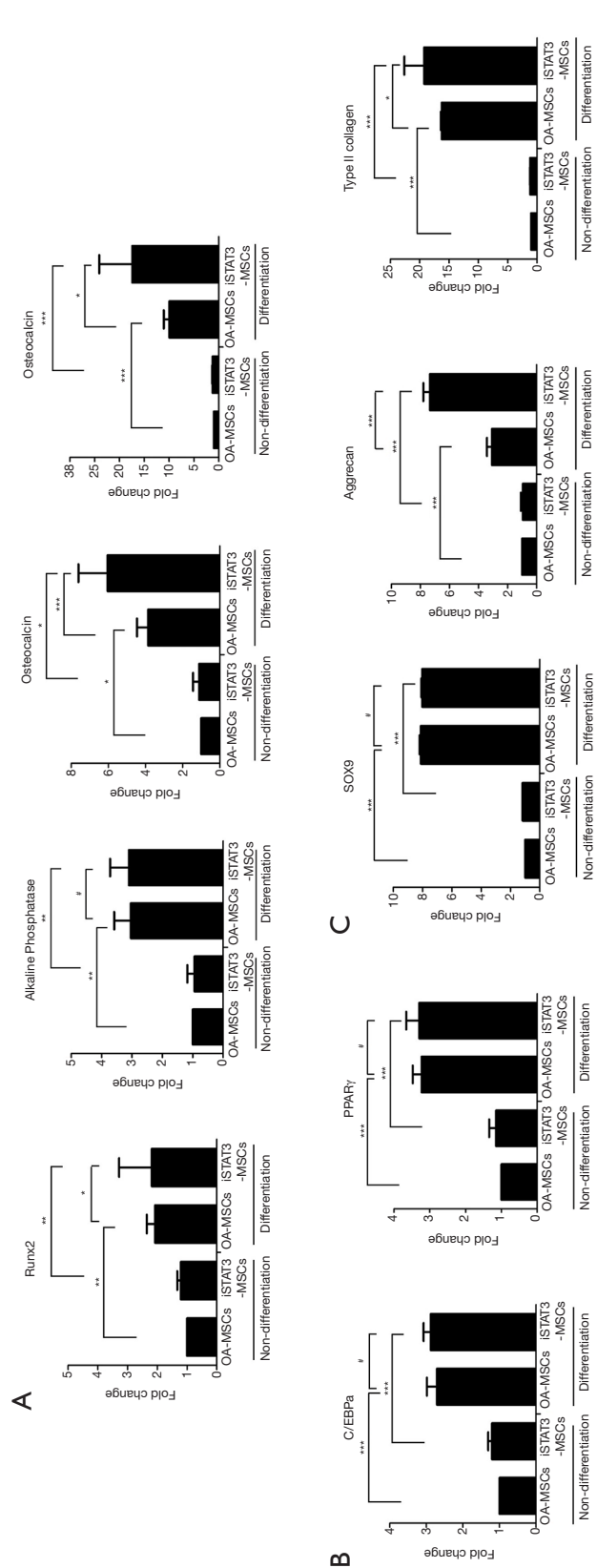
Figure 6 Comparative gene expression analysis. (A) Expression levels of osteogenic differentiation markers (*RUNX2*, alkaline phosphatase, osteocalcin, and osteopontin), 14 days after osteogenic differentiation. The expression of *RUNX2*, alkaline phosphatase, osteocalcin, and osteopontin was higher in differentiated than undifferentiated OA-MSCs and iSTAT3-MSCs (*, P<0.05; **, P<0.01; ***, P<0.001). The expression of all of these genes, except *ALP* (#, P>0.05), also differed between differentiated OA-MSCs and iSTAT3-MSCs (*, P<0.05; ***, P<0.001). (B) The expression of adipogenic differentiation genes (*C/EBPα* and *PPARγ*), 14 days after adipogenic differentiation. The expression of *C/EBPα* and *PPARγ* was higher in differentiated than undifferentiated cells (***, P<0.001). However, no significant differences in *C/EBPα* and *PPARγ* expression levels were detected between differentiated OA-MSCs and iSTAT3-MSCs (#, P>0.05). (C) The expression of chondrogenic differentiation markers (*SOX9*, aggrecan, and type II collagen), 21 days after chondrogenic differentiation. The expression levels of *SOX9*, aggrecan, and type II collagen were higher in differentiated than undifferentiated OA-MSCs and iSTAT3-MSCs (***, P<0.001). Additionally, the expression of *SOX9*, aggrecan, and type II collagen was different between OA-MSCs and iSTAT3-MSCs in the differentiated state (#, P>0.05; *, P<0.05; ***, P<0.001). OA-MSCs, mesenchymal stem cells in patients with osteoarthritis; STAT3, signal transducer and activator of transcription 3.
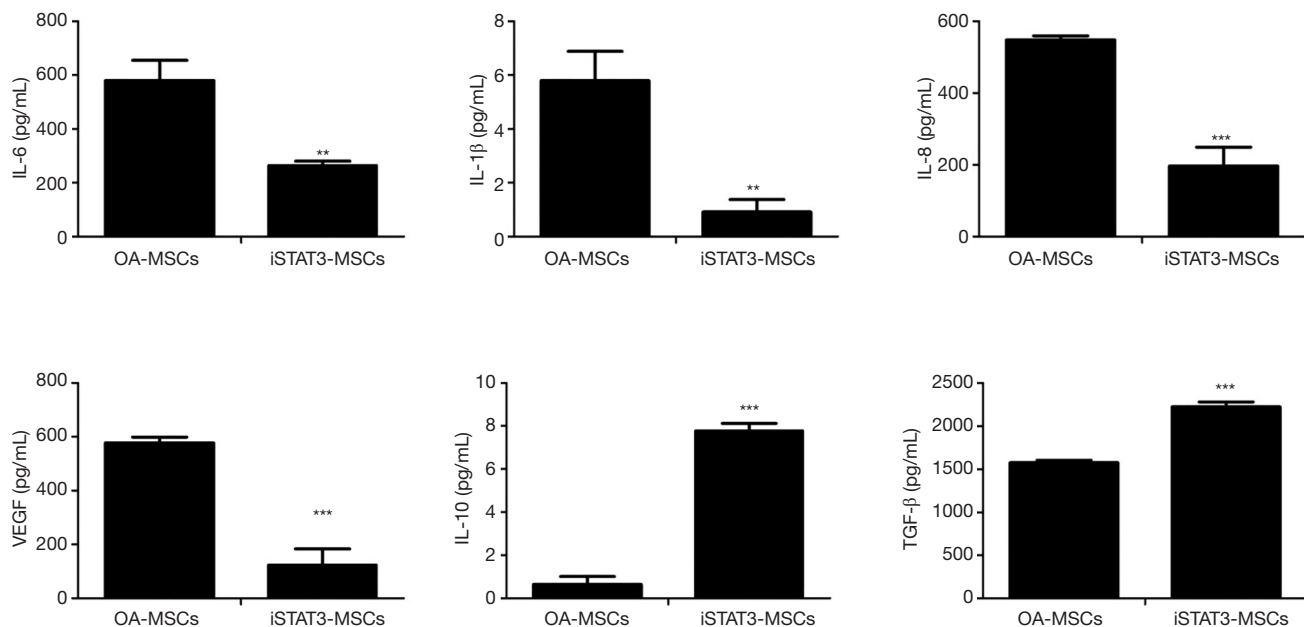
Figure 7 Anti-inflammatory activity of iSTAT3-MSCs. The expression level of pro-inflammatory cytokines including IL-6, IL-1β, IL-8, and VEGF, were significantly lower in the supernatants of iSTAT3-MSCs (**, P<0.01, ***, P<0.001). In contrast, the levels of the anti-inflammatory cytokines, IL-10 and TGF-β, were significantly higher in the culture supernatants of iSTAT3-MSCs (***, P<0.001). STAT3, signal transducer and activator of transcription 3; MSCs, mesenchymal stem cells.

of iSTAT3-MSCs, which showed 2.88-fold and 3.3-fold higher expression in differentiated than undifferentiated cells (*Figure 6B*; ***, P<0.001). However, there were no significant differences in *C/EBPα* and *PPARγ* expression levels between differentiated OA-MSCs and iSTAT3-MSCs (*Figure 6B*; #, P>0.05).

Moreover, with respect to chondrogenic differentiation-specific markers, the expression levels of *SOX9*, aggrecan, and type II collagen were higher in differentiated than undifferentiated OA-MSCs (8.13-fold, 3.08-fold, and 16.26-fold, respectively) and iSTAT3-MSCs (7.08-fold, 7.35-fold, and 19.24-fold, respectively) (*Figure 6C*; ***, P<0.001). Additionally, there were significant differences in the expression levels of aggrecan and type II collagen between OA-MSCs and iSTAT3-MSCs (*Figure 6C*; *, P<0.05 and ***, P<0.001). But, the expression level of *SOX9* was not significant between OA-MSCs and iSTAT3-MSCs (*Figure 6C*; #, P>0.05).

Inhibition of STAT3 signaling induces the anti-inflammatory response of OA-MSCs

The levels of different cytokines in the culture supernatants of OA-MSCs and iSTAT3-MSCs were evaluated using ELISA (*Figure 7*). The levels of pro-inflammatory cytokines, including IL-6, IL-1β, IL-8, and VEGF, were significantly lower in the supernatants of iSTAT3-MSCs than in those of OA-MSCs (IL-6 and IL-1β; **, P<0.01; IL-8 and VEGF; ***, P<0.001). In contrast, the levels of the anti-inflammatory cytokines, IL-10 and TGF-β, were significantly higher in the culture supernatants of iSTAT3-MSCs than in those of OA-MSCs (***, P<0.001). Altogether, these data show that STAT3 signaling inhibition may increase the anti-inflammatory response and improve the therapeutic effects of MSCs.

Discussion

Stem cells collected from different sources, including the bone marrow, adipose tissue, cord blood, and synovium have clearly established clinical applications (22-24). To utilize autologous cells, surgical or invasive procedures are necessary to obtain the tissues. Traditionally, the bone marrow has been an important source of stem cells; however, bone marrow aspiration is a very painful procedure (25). Nevertheless, clinical studies with bone marrow aspirates are ongoing owing to their simple culture process and favorable stemness characteristics (26-29).

Additionally, large numbers of cells can be isolated from the adipose tissues, with a higher chondrogenic potential than MSCs from other sources; however, an invasive procedure is still required to harvest these cells (30,31). To avoid such procedures, allogenic cells are a commercially available alternative. Nonetheless, it is difficult and time-consuming to obtain approval from the FDA and there are many ethical concerns associated (32).

HVB can be obtained easily after bone surgery, such as TKA, without special procedures, pain, or related ethical issues. The volume of HVB obtained varies among patients; nevertheless, a sufficient number of MSCs can be obtained by concentration and cultivation. Accordingly, HVB is a potential stem cell source. Importantly, HVB has bone marrow components, although stromal components are less abundant in these samples than in bone marrow aspirates. However, the issue of low numbers of stem cells or stromal cells in HVB can be resolved by repeated concentration after sample collection following TKA. As the stromal component of the bone marrow can be used for the treatment of musculoskeletal diseases, centrifugation and concentration of the stromal component are inevitable.

The hemovac allows the collection of up to 400 mL of blood; the kit used in this study handled a volume of 40 mL. Theoretically, 800 mL from the first and second hemovac drains can be concentrated (8). Contrastingly, the contents of the third hemovac drain are dominated by venous blood; therefore, concentration is not effective. Notably, through the method used in this study, it is possible to produce 4 mL of HVBC and obtain 20-fold increased cell counts, allowing the culture of HVBC cells for clinical applications.

OA is a degenerative joint disease that presents with inflammation and, consequently, with elevated levels of proinflammatory cytokines (33,34). MSCs can modulate the inflammatory response; nonetheless, their application for the treatment of OA may be associated with a few problems (35,36). For instance, it has been reported that MSCs can differentiate into several proinflammatory cells, failing to decrease the inflammatory immune response (37). Therefore, the development of optimization strategies to regulate the immunomodulatory function of MSCs, such as the inhibition of STAT3 signaling, may be necessary before the clinical application of MSCs in the treatment of OA can be implemented.

A concern regarding this newly developed method is that the quality of stem cells from old individuals and patients with severe inflammation may be low (38-40). STAT3 is a transcription factor belonging to the STAT protein family (41,42) that is activated by inflammatory cytokines, including in diseases associated with chronic inflammation and fibrosis (42-47). The restoration of stem cell function by STAT3 signaling inhibition has been previously evaluated (48-51). For instance, STAT3 signaling inhibition in MSCs from the adipose tissue resulted in improved anti-inflammatory response and reduced inflammation (50). Reduced OA severity in a rat model and pain relief have also been reported (50). However, these studies were based on cells from the adipose tissue or other sources; studies using HVBs have not been conducted to date. Notably, the stem cell characteristics or function could differ according to the source or environmental conditions of the harvested tissue (e.g., with respect to age and degree of inflammation) (20,37,52,53).

Importantly, to consider the use of STAT3 signaling-suppressed HVB cells for stem cell research, three key points must be addressed. First, stem cell marker expression should be maintained to ensure the lack of changes in the characteristics of stem cells after STAT3 signaling suppression. In this study, we showed that iSTAT3-MSCs maintained the expression levels of stem cell markers (high expression of CD73, CD90, and CD105) as well as the fibroblast-like morphology observed in the context of the "mother cells" (OA-MSCs) (*Figures 2,3*). Therefore, these results suggest the above pre-requisite can be fulfilled.

Second, iSTAT3-MSCs should maintain a multi-lineage differentiation potential. In this study, the osteogenic, adipogenic, and chondrogenic differentiation potentials of OA-MSCs and iSTAT3-MSCs were evaluated (*Figure 4,5*). Higher expression levels of *RUNX2*, *ALP*, osteocalcin, and osteopontin (osteogenic markers) were observed in OA-MSCs and iSTAT3-MSCs in the differentiated state than in the undifferentiated state (*Figure 6A*). Additionally, the ALP activity (*Figure 4A*) and Alizarin red S staining intensity (calcium deposition and mineralization; *Figure 4B*) of OA-MSCs and iSTAT3-MSCs were higher in differentiated than undifferentiated cells. Moreover, the expression of *PPARγ* and *C/EBPα*, adipocyte differentiation marker levels (*Figure 6B*), and lipid droplet formation (as per Oil red O staining) were increased in differentiated OA-MSCs and iSTAT3-MSCs (*Figure 4C*). The same was true in the context of the expression of different chondrogenic markers, including *SOX9*, aggrecan, and type II collagen (*Figure 6C*) as well as Alcian blue (pH 2.5), toluidine blue, and type II collagen staining (*Figure 5*). Altogether, these results support the notion that iSTAT3-MSCs show a multi-lineage differentiation potential. Interestingly,

Page 12 of 14

Lee et al. STAT3 suppression in MSCs from HVB

both osteogenic and chondrogenic potentials were higher in iSTAT3-MSCs than in OA-MSCs (*Figure 6A,6C*). Therefore, our data support the future clinical applications of iSTAT3-MSCs. If iSTAT3-MSCs, generated after TKA surgery are stored in a freezer, they can be used to resolve bone disorders, including fractures, non-union fractures, and avascular necrosis (51,54-56). Furthermore, since after TKA, patients mainly use the non-operated leg, which can lead to injury in the articular cartilage of the knee joint, iSTAT3-MSCs, with enhanced chondrogenic potential, can be used to treat potential cartilage defects of non-operated knees.

Third, similar to iSTAT3-MSCs from other sources, such as the adipose tissue (50) anti-inflammatory properties must be demonstrated. Here, iSTAT3-MSCs obtained from HVBCs showed lower pro-inflammatory and higher anti-inflammatory activity than OA-MSCs, as per the determined cytokine levels (*Figure* 7). Therefore, these results indicate that STAT3 suppression is effective for the optimization of MSCs isolated in the context of inflammatory and degenerative conditions.

To the best of our knowledge, no studies on MSCs with STAT3 signaling suppression derived from HVB have been conducted to date. Overall, the results of the current study show the advantages of iSTAT3-MSCs over OA-MSCs with respect to osteogenic and chondrogenic differentiation ability as well as anti-inflammatory potential. Therefore, in conclusion, our results suggest that iSTAT3-MSCs obtained from HBV after TKA are promising for stem cell research purposes and the treatment of musculoskeletal diseases.

Acknowledgments

Footnote

Reporting Checklist: The authors have completed the MDAR reporting checklist. Available at https://dx.doi.org/10.21037/atm-21-791

Data Sharing Statement: Available at https://dx.doi.org/10.21037/atm-21-791

Conflicts of Interest: All authors have completed the ICMJE uniform disclosure form (available at https://dx.doi.org/10.21037/atm-21-791). The authors have no conflicts of interest to declare.

Ethical Statement: The authors are accountable for all aspects of the work in ensuring that questions related to the accuracy or integrity of any part of the work are appropriately investigated and resolved. The study was conducted in accordance with the Declaration of Helsinki (as revised in 2013). The study was approved by the Institutional Review Board of Uijeongbu St. Mary's Hospital, Korea (UC18DESI0056) and informed consent was obtained from all participants.

Open Access Statement: This is an Open Access article distributed in accordance with the Creative Commons Attribution-NonCommercial-NoDerivs 4.0 International License (CC BY-NC-ND 4.0), which permits the non-commercial replication and distribution of the article with the strict proviso that no changes or edits are made and the original work is properly cited (including links to both the formal publication through the relevant DOI and the license). See: https://creativecommons.org/licenses/by-nc-nd/4.0/.

References

1. Dalury DF. Cementless total knee arthroplasty: current concepts review. Bone Joint J 2016;98-B:867-73.
2. Cram P, Lu X, Kates SL, et al. Total knee arthroplasty volume, utilization, and outcomes among Medicare beneficiaries, 1991-2010. JAMA 2012;308:1227-36.
3. Mandl LA, Martin GM, Hunter D, et al. Overview of surgical therapy of knee and hip osteoarthritis. Waltham, MA: UpToDate.
4. Higashi H, Barendregt JJ. Cost-effectiveness of total hip and knee replacements for the Australian population with osteoarthritis: discrete-event simulation model. PLoS One 2011;6:e25403.
5. Kelly MP, Prentice HA, Wang W, et al. Reasons for Ninety-Day Emergency Visits and Readmissions After Elective Total Joint Arthroplasty: Results From a US Integrated Healthcare System. J Arthroplasty 2018;33:2075-81.
6. Lee SH, Kim DH, Lee YS. Is there an optimal age for total knee arthroplasty? A systematic review. Knee Surg Relat Res 2020;32:60.
7. Scranton PE Jr. Management of knee pain and stiffness after total knee arthroplasty. J Arthroplasty 2001;16:428-35.
8. Levy O, Martinowitz U, Oran A, et al. The use of fibrin

tissue adhesive to reduce blood loss and the need for blood transfusion after total knee arthroplasty. A prospective, randomized, multicenter study. J Bone Joint Surg Am 1999;81:1580-8.

9. Pornrattanamaneewong C, Narkbunnam R, Siriwattanasakul P, et al. Three-hour interval drain clamping reduces postoperative bleeding in total knee arthroplasty: a prospective randomized controlled trial. Arch Orthop Trauma Surg 2012;132:1059-63.

10. Li MM, Kwok JY, Chung KY, et al. Prospective randomized trial comparing efficacy and safety of intravenous and intra-articular tranexamic acid in total knee arthroplasty. Knee Surg Relat Res 2020;32:62.

11. Lee SH, Kim JI, Choi W, et al. Effectiveness of iron supplementation in the perioperative management of total knee arthroplasty: a systematic review. Knee Surg Relat Res 2020;32:44.

12. Basaran H, Dasar U, Satılmış B, et al. Usage of Positive pressure Hemovac Drain following Total Knee Arthroplasty: Reduce Blood Lossor Not. SM J Orthop 2016;2:1027.

13. Jaafar S, Vigdorchik J, Markel DC. Drain technique in elective total joint arthroplasty. Orthopedics 2014;37:37-9.

14. Park D, Choi YH, Cho KH, et al. 3-h drain clamping is not effective to reduce total blood loss after primary total knowledge. Knee Surg Relat Res 2020;32:33.

15. Lee DH, Kong CG, Shin YW, et al. Which is better for articular cartilage regeneration, cultured stem cells or concentrated stromal cells? Ann Transl Med 2020;8:836.

16. Bianco P, Riminucci M, Gronthos S, et al. Bone marrow stromal stem cells: nature, biology, and potential applications. Stem Cells 2001;19:180-92.

17. Kim SA, Park HY, Shin YW, et al. Hemovac blood after total knee arthroplasty as a source of stem cells. Ann Transl Med 2020;8:1406.

18. Arden N, Nevitt MC. Osteoarthritis: epidemiology. Best Pract Res Clin Rheumatol 2006;20:3-25.

19. Hwang IY, Park KB, Chang SW, et al. Preoperative vitamin D level does not affect the short-term functional outcome after total knee arthroplasty in elderly women. Knee Surg Relat Res 2020;32:30.

20. Waterman RS, Tomchuck SL, Henkle SL, et al. A new mesenchymal stem cell (MSC) paradigm: polarization into a pro-inflammatory MSC1 or an Immunosuppressive MSC2 phenotype. PLoS One 2010;5:e10088.

21. Avery MB, Belanger BL, Bromley A, et al. Mesenchymal Stem Cells Exhibit Both a Proinflammatory and Anti-Inflammatory Effect on Saccular Aneurysm Formation in a

Rabbit Model. Stem Cells Int 2019;2019:3618217.

22. Jin HJ, Bae YK, Kim M, et al. Comparative analysis of human mesenchymal stem cells from bone marrow, adipose tissue, and umbilical cord blood as sources of cell therapy. Int J Mol Sci 2013;14:17986-8001.

23. Jeon YJ, Kim J, Cho JH, et al. Comparative Analysis of Human Mesenchymal Stem Cells Derived From Bone Marrow, Placenta, and Adipose Tissue as Sources of Cell Therapy. J Cell Biochem 2016;117:1112-25.

24. Peng L, Jia Z, Yin X, et al. Comparative analysis of mesenchymal stem cells from bone marrow, cartilage, and adipose tissue. Stem Cells Dev 2008;17:761-73.

25. Barberi T, Willis LM, Socci ND, et al. Derivation of multipotent mesenchymal precursors from human embryonic stem cells. PLoS Med 2005;2:e161.

26. Murray IR, Robinson PG, West CC, et al. Reporting Standards in Clinical Studies Evaluating Bone Marrow Aspirate Concentrate: A Systematic Review. Arthroscopy 2018;34:1366-75.

27. Madry H, Gao L, Eichler H, et al. Bone Marrow Aspirate Concentrate-Enhanced Marrow Stimulation of Chondral Defects. Stem Cells Int 2017;2017:1609685.

28. Piuzzi NS, Hussain ZB, Chahla J, et al. Variability in the Preparation, Reporting, and Use of Bone Marrow Aspirate Concentrate in Musculoskeletal Disorders: A Systematic Review of the Clinical Orthopaedic Literature. J Bone Joint Surg Am 2018;100:517-25.

29. Gianakos AL, Sun L, Patel JN, et al. Clinical application of concentrated bone marrow aspirate in orthopaedics: A systematic review. World J Orthop 2017;8:491-506.

30. Francis SL, Duchi S, Onofrillo C, et al. Adipose-Derived Mesenchymal Stem Cells in the Use of Cartilage Tissue Engineering: The Need for a Rapid Isolation Procedure. Stem Cells Int 2018;2018:8947548.

31. Huri PY, Hamsici S, Ergene E, et al. Infrapatellar Fat Pad-Derived Stem Cell-Based Regenerative Strategies in Orthopedic Surgery. Knee Surg Relat Res 2018;30:179-86.

32. Lo B, Parham L. Ethical issues in stem cell research. Endocr Rev 2009;30:204-13.

33. Chow YY, Chin KY. The Role of Inflammation in the Pathogenesis of Osteoarthritis. Mediators Inflamm 2020;2020:8293921.

34. Goldring MB. Osteoarthritis and cartilage: the role of cytokines. Curr Rheumatol Rep 2000;2:459-65.

35. Theeuwes WF, van den Bosch MHJ, Thurlings RM, et al. The role of inflammation in mesenchymal stromal cell therapy in osteoarthritis, perspectives for post-traumatic osteoarthritis: a review. Rheumatology (Oxford)

Page 14 of 14

Lee et al. STAT3 suppression in MSCs from HVB

2021;60:1042-53.

36. Kim GB, Shon OJ. Current perspectives in stem cell therapies for osteoarthritis of the knee. Yeungnam Univ J Med 2020;37:149-58.

37. Inoue S, Popp FC, Koehl GE, et al. Immunomodulatory effects of mesenchymal stem cells in a rat organ transplant model. Transplantation 2006;81:1589-95.

38. Lin H, Sohn J, Shen H, et al. Bone marrow mesenchymal stem cells: Aging and tissue engineering applications to enhance bone healing. Biomaterials 2019;203:96-110.

39. Oh J, Lee YD, Wagers AJ. Stem cell aging: mechanisms, regulators and therapeutic opportunities. Nat Med 2014;20:870-80.

40. Li TS, Kubo M, Ueda K, et al. Impaired angiogenic potency of bone marrow cells from patients with advanced age, anemia, and renal failure. J Thorac Cardiovasc Surg 2010;139:459-65.

41. Zhong Z, Wen Z, Darnell JE Jr. Stat3: a STAT family member activated by tyrosine phosphorylation in response to epidermal growth factor and interleukin-6. Science 1994;264:95-8.

42. Hillmer EJ, Zhang H, Li HS, et al. STAT3 signaling in immunity. Cytokine Growth Factor Rev 2016;31:1-15.

43. Kasembeli MM, Bharadwaj U, Robinson P, et al. Contribution of STAT3 to Inflammatory and Fibrotic Diseases and Prospects for its Targeting for Treatment. Int J Mol Sci 2018;19:2299.

44. Zhao J, Qi YF, Yu YR. STAT3: A key regulator in liver fibrosis. Ann Hepatol 2021;21:100224.

45. Knight D, Mutsaers SE, Prêle CM. STAT3 in tissue fibrosis: is there a role in the lung? Pulm Pharmacol Ther 2011;24:193-8.

46. Cheng C, Shan W, Huang W, et al. ACY-1215 exhibits anti-inflammatory and chondroprotective effects in human osteoarthritis chondrocytes via inhibition of STAT3 and NF-κB signaling pathways. Biomed Pharmacother 2019;109:2464-71.

47. Fan Y, Mao R, Yang J. NF-κB and STAT3 signaling pathways collaboratively link inflammation to cancer. Protein Cell 2013;4:176-85.

48. Sherry MM, Reeves A, Wu JK, et al. STAT3 is required for proliferation and maintenance of multipotency in glioblastoma stem cells. Stem Cells 2009;27:2383-92.

49. Cui X, Liu J, Bai L, et al. Interleukin-6 induces malignant transformation of rat mesenchymal stem cells in association with enhanced signaling of signal transducer and activator of transcription 3. Cancer Sci 2014;105:64-71.

50. Lee SY, Lee SH, Na HS, et al. The Therapeutic Effect of STAT3 Signaling-Suppressed MSC on Pain and Articular Cartilage Damage in a Rat Model of Monosodium Iodoacetate-Induced Osteoarthritis. Front Immunol 2018;9:2881.

51. Shu P, Sun DL, Shu ZX, et al. Therapeutic Applications of Genes and Gene-Engineered Mesenchymal Stem Cells for Femoral Head Necrosis. Hum Gene Ther 2020;31:286-96.

52. Gibon E, Lu L, Goodman SB. Aging, inflammation, stem cells, and bone healing. Stem Cell Res Ther 2016;7:44.

53. Dufrane D. Impact of Age on Human Adipose Stem Cells for Bone Tissue Engineering. Cell Transplant 2017;26:1496-504.

54. Zhao D, Cui D, Wang B, et al. Treatment of early stage osteonecrosis of the femoral head with autologous implantation of bone marrow-derived and cultured mesenchymal stem cells. Bone 2012;50:325-30.

55. El-Jawhari JJ, Kleftouris G, El-Sherbiny Y, et al. Defective Proliferation and Osteogenic Potential with Altered Immunoregulatory phenotype of Native Bone marrow-Multipotential Stromal Cells in Atrophic Fracture Non-Union. Sci Rep 2019;9:17340.

56. Granero-Moltó F, Weis JA, Miga MI, et al. Regenerative effects of transplanted mesenchymal stem cells in fracture healing. Stem Cells 2009;27:1887-98.